GA–A27399

IMPROVED UNDERSTANDING OF PHYSICS PROCESSES IN PEDESTAL STRUCTURE, LEADING TO IMPROVED PREDICTIVE CAPABILITY FOR ITER

by
R.J. GROEBNER, C.S. CHANG, J.W. HUGHES, R. MAINGI, P.B. SNYDER,
X.Q. XU, E.A. BELLI, B.D. BRAY, J. CANDY, T.M. DETERLY, N.M. FERRARO,
J.E. KINSEY, A.W. LEONARD, C. LIU, T.H. OSBORNE, D.M. PONCE, S.P. SMITH,
G.M. STAEBLER, R.E. WALTZ, W.M. STACEY, M.E. FENSTERMACHER, I. JOSEPH,
C.J. LASNIER, M.V. UMANSKY, E.H-J. WANG, R.M. CHURCHILL, I. CZIEGLER,
E.M. DAVIS, A.E. HUBBARD, B. LaBOMBARD, B.L. LIPSCHULTZ, Y. MA,
J.C. ROST, L.E. SUGIYAMA, J.L. TERRY, J. WALK, A.E. WHITE, D.G. WHYTE,
S.M. WOLFE, J.M. CANIK, J.D. LORE, A.C. SONTAG, D.P. BOYLE, A. DIALLO,
S.J. ZWEBEN, J.G. WATKINS, A.Y. PANKIN, D.P. FULTON, Z. LIN, E.J. DOYLE,
T.L. RHODES, L. SCHMITZ, L. ZENG, J.A. BOEDO, P.H. DIAMOND,
D.P. ELDON, S.E. PARKER, W. WAN, J.D. ELDER,
J.D. CALLEN, G.R. McKEE and Z. YAN

SEPTEMBER 2012

GENERAL ATOMICS

DISCLAIMER

GA–A27399

IMPROVED UNDERSTANDING OF PHYSICS PROCESSES IN PEDESTAL STRUCTURE, LEADING TO IMPROVED PREDICTIVE CAPABILITY FOR ITER

by
R.J. GROEBNER, C.S. CHANG,[1] J.W. HUGHES,[2] R. MAINGI,[3] P.B. SNYDER,
X.Q. XU,[4] E.A. BELLI, B.D. BRAY, J. CANDY, T.M. DETERLY, N.M. FERRARO,
J.E. KINSEY, A.W. LEONARD, C. LIU, T.H. OSBORNE, D.M. PONCE, S.P. SMITH,
G.M. STAEBLER, R.E. WALTZ, W.M. STACEY,[5] M.E. FENSTERMACHER,[4] I. JOSEPH,[4]
C.J. LASNIER,[4] M.V. UMANSKY,[4] E.H-J. WANG,[4] R.M. CHURCHILL,[2] I. CZIEGLER,[2]
E.M. DAVIS,[2] A.E. HUBBARD,[2] B. LaBOMBARD,[2] B.L. LIPSCHULTZ,[2] Y. MA,[2]
J.C. ROST,[2] L.E. SUGIYAMA,[2] J.L. TERRY,[2] J. WALK,[2] A.E. WHITE,[2] D.G. WHYTE,[2]
S.M. WOLFE,[2] J.M. CANIK,[3] J.D. LORE,[3] A.C. SONTAG,[3] D.P. BOYLE,[1] A. DIALLO,[1]
S.J. ZWEBEN,[1] J.G. WATKINS,[6] A.Y. PANKIN,[7] D.P. FULTON,[8] Z. LIN,[8] E.J. DOYLE,[9]
T.L. RHODES,[9] L. SCHMITZ,[9] L. ZENG,[9] J.A. BOEDO,[10] P.H. DIAMOND,[10]
D.P. ELDON,[10] S.E. PARKER,[11] W. WAN,[11] J.D. ELDER,[12]
J.D. CALLEN,[13] G.R. McKEE[13] and Z. YAN[13]

This is a preprint of a paper to be presented at the 24th IAEA Fusion Energy Conference, October 8–13, 2012 in San Diego, California and to be published in the Proceedings.

[1]Princeton Plasma Physics Laboratory, Princeton, NJ USA
[2]Massachusetts Institute of Technology, Cambridge, MA USA
[3]Oak Ridge National Laboratory, Oak Ridge, TN USA
[4]Lawrence Livermore National Laboratory, Livermore, CA USA
[5]Georgia Institute of Technology, Atlanta, GA 30332
[6]Sandia National Laboratory, Albuquerque, NM USA
[7]Tech-X, Boulder, CO USA
[8]U. California-Irvine, Irvine, CA USA
[9]U. California-Los Angeles, Los Angeles, CA USA
[10]U. California San Diego, La Jolla, CA USA
[11]University of Colorado at Boulder, Boulder, CO 80309
[12]U. Toronto Institute for Aerospace Studies, Toronto, Ontario, Canada
[13]U. Wisconsin-Madison, Madison, WI USA

Work supported by the U.S. Department of Energy under
DE-FC02-04ER54698, DE-FG02-95ER54309, DE-FG02-00ER54538, DE-AC52-07NA27344,
DE-FC02-93ER54186, DE-AC05-00OR22725, DE-AC02-09CH11466, DE-AC04-94AL85000,
DE-FG03-94ER54271, DE-FG02-08ER54984, DE-FG02-07ER54917, DE-FC02-05ER54816,
DE-FG02-89ER53296 and DE-FG02-08ER54999

GENERAL ATOMICS PROJECT 30200
SEPTEMBER 2012

GENERAL ATOMICS

ABSTRACT

Joint experiment/theory/modeling research has led to increased confidence in predictions of the pedestal height in ITER. This work was performed as part of a US DOE Joint Research Target in FY11 to identify physics processes that control the H-mode pedestal structure. The study included experiments on C-Mod, DIII-D and NSTX as well as interpretation of experimental data with theory-based modeling codes. This work provides increased confidence in the ability of models for peeling-ballooning stability, bootstrap current, pedestal width scaling and pedestal height to make correct predictions, with some areas needing further work also being identified. A model for pedestal pressure height has made good predictions in existing machines for a range in pressure of a factor of 20. There is a good basis that the pedestal pressure height in ITER can be predicted with an accuracy of about 20%. Models were studied for a number of processes that are proposed to play a role in the pedestal n_e and T_e profiles. These processes include neoclassical transport, paleoclassical transport, electron temperature gradient turbulence and neutral fuelling. All of these processes may be important, with the importance being dependent on the plasma regime.

1. INTRODUCTION

The H-mode pedestal will have a profound effect on plasma performance in ITER [1], FNSF [2] and other fusion machines, and the characteristics of these pedestals must be optimized in several ways for these devices to succeed. These characteristics include sufficient pedestal pressure, small or no ELMs, shielding of impurities and the ability to be fuelled by gas or pellet injection. A predictive pedestal capability is required to optimize and design operating scenarios in ITER and to assist in the design of future fusion machines so that the pedestals can be modeled with realistic properties. To assist with the development of predictive capability, the US Department of Energy established an activity in fiscal year 2011, called the Joint Research Target (JRT) to foster an increased effort to study pedestal physics. This activity resulted in a coordinated effort between experiment, theory and modeling to identify and improve predictive capability for important physics processes controlling pedestal structure. This work has led to increased confidence in the ability of quantitative models to correctly compute limits to pedestal evolution set by MHD stability, to compute the bootstrap current driven by pedestal pressure gradients, to compute pedestal width and to predict the pedestal pressure height in current machines and in ITER. The effort examined several physics processes that are proposed to control temperature and density profiles. The results indicate that several processes probably play a role in pedestal structure and models will need to include multiple processes in a self-consistent way to make correct predictions.

2. LIMITS TO PEDESTAL PRESSURE

2.1 PEELING-BALLOONING LIMITS TO MAXIMUM PRESSURE

It has been known for some time that the peeling-ballooning (PB) theory predicts the observed boundary for instability to Type I ELMs on a number of machines [3]. It has also been empirically observed that peeling-ballooning physics provides the ultimate limits to attainable pedestal pressure in the H-mode regime. Models based on PB theory are able to correctly determine if a given set of pedestal temperature and density profiles are realizable in a device. Models of peeling-ballooning modes have been extended for applications to the compact, high-field C-Mod device and the low-field, low aspect ratio NSTX device. Peeling-ballooning stability analysis of Type-I ELMing regimes and regimes in which ELMs were suppressed or not observed was performed on all three machines. The results support the premise that these models are able to quantitatively predict the limits to the pedestal pressure.

In these studies and other experimental studies reported here, a standard analysis methodology was adopted to process and compare data from C-Mod, DIII-D and NSTX. The analysis workflow was to: obtain measurements of pedestal T_e and n_e profiles from high resolution Thomson scattering systems; obtain measurements of pedestal T_i and low-Z impurity density with high resolution charge exchange recombination spectroscopy when available; obtain magnetic equilibria with the EFIT [4] code; use a set of python software tools to fit analytic functions to edge profile data [5]; generate "kinetic" equilibria with the EFIT code where the pressure profile was constrained by experimental measurements and the edge bootstrap current was calculated from experimental measurements with an analytic model, such as the Sauter [6] model. For calculations of peeling-ballooning thresholds, a series of Grad-Shafranov equilibria were generated to map out a space of pedestal pressure gradient and current density by perturbing the pressure and current density profiles used to represent the actual experiment.

The ELITE [7] code has been run on these equilibria, typically for mode numbers in the range n=5–30, to map out parameter regimes that are stable and unstable to PB modes. For the moderate aspect ratio machines, DIII-D and C-Mod, the threshold for instability is obtained from the criterion $\gamma / \omega_\alpha > 0.05$, where ω_α is the Alfven frequency and γ is the linear growth rate for the fastest growing peeling-ballooning mode. For application of ELITE to C-Mod, a simple model of diamagnetic stabilization was added to the code due to the fact that diamagnetic effects are important in this high field machine. For application to NSTX, the threshold condition for ELM onset was taken as $\gamma / \omega_{*pi} > 0.05$, where ω_{*pi} is the ion diamagnetic drift frequency. A number of Type I ELMing discharges from all three machines were analyzed in this way and the experimental operating points near the onset of the ELMs were found to be within error bars of the computed threshold for instability to PB modes. As an example, Fig. 1 shows that the ELITE code predicts peeling-ballooning stability very near the measured operating points in matched Type-I ELMing discharges in C-Mod and DIII-D.

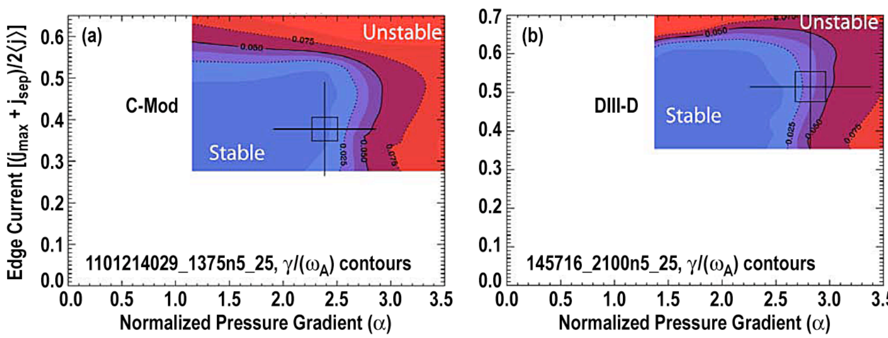

Fig. 1. Peeling-ballooning stability diagrams calculated with ELITE for (a) Alcator C-Mod shot 1101214029, and (b) DIII-D shot 145716. These discharges are near dimensionless similarity, with the DIII-D discharge run in the typical Alcator C-Mod ELMing shape. The crosshair shows the experimental operating point location, obtained just before a Type I ELM. Solid contour represents threshold for instability.

Pedestals that clearly lie in the predicted unstable regions have not been observed in this work. However, all three machines observed good confinement regimes without ELMs that operated at or below the predicted PB threshold. Stability analysis of DIII-D discharges showed that the QH-mode regime operates near the PB threshold and the ELM-suppressed regimes obtained with the application of resonant magnetic perturbations lie below the limit [5]. ELM-free regimes in NSTX obtained with the application of lithium coatings operated below the PB limit [8]. In C-Mod, discharges in the I-mode regime exhibit H-mode like gradients in T_e, L-mode like gradients in n_e and operate well below the predicted PB limit. EDA discharges in C-Mod operate close to but below the PB threshold. In summary, peeling-ballooning theory provides an upper limit to the attainable pedestal pressure in the experiments performed in these machines.

2.2 COMPARISON OF MODELS OF BOOTSTRAP CURRENT

Large pressure gradients in the pedestal drive an edge bootstrap current. This current plays an important role in the physics of peeling-ballooning modes and must be known accurately in order to compute the stability threshold. The magnetic shear, strongly modified by the bootstrap current, is also an important quantity in several pedestal transport models. The bootstrap current is computed from theoretical neoclassical models, such as the Sauter analytic model [6] or the NCLASS model [9] for use in models of peeling-ballooning stability. Due to the important role of the bootstrap current, it is important that these theoretical models be validated, preferably against experiment. There have been some measurements of bootstrap current on DIII-D [10] and MAST [11] and neoclassical models have been found to be in close agreement with these measurements in steady state.

In the JRT activity, there was significant work to benchmark more complete models for the bootstrap current against the simpler models in general use. This work was done with the XGC0 [12] and NEO [13] codes, which perform kinetic calculations in realistic geometry. In brief, these comparisons found that the simpler models are often accurate to better than 10%, but significant variations from the simpler models were found for some conditions.

Calculations with XGC0 find that for pedestals in the banana-plateau collisionality regime, the analytic Sauter formula calculation of bootstrap current agrees well with the numerical calculations. However, when the pedestal electrons are in the collisional regime, the numerical simulation yields approximately 15–20% lower bootstrap current in a conventional tokamak, and approximately 30% higher bootstrap current in a low aspect ratio tokamak [14]. Calculations with NEO including the full linearized Fokker-Planck collision operator and a carbon impurity find small but significant (~10–20%) differences in the bootstrap current from that calculated in simplified models such as NCLASS or Sauter.

2.3 PEDESTAL WIDTH SCALING

Pedestal width measurements from all three machines have been used to test a model of width scaling, based on the hypothesis that kinetic ballooning modes (KBMs) limit the pedestal pressure gradient when it reaches a critical value [15]. To leading order, the physics in the model implies that the pedestal width Δ scales as $\Delta=c(\beta_{\theta,ped})^{1/2}$ where $\beta_{\theta,ped}$ is the pedestal beta poloidal and c is a constant of about 0.1 [15]. The width in this scaling is defined as the average of the T_e and n_e widths, evaluated with fits of a tanh function to the pedestal profiles.

For all three machines, this scaling relationship was found to be a good description of the measured scaling. For the moderate aspect ratio machines C-Mod [16] and DIII-D [15,17], the best values of c are nearly identical, 0.088 and 0.076 respectively. For the low aspect ratio NSTX [18] device, the best value of c is 0.17. Thus, all three machines show evidence that the same underlying physics controls the width scaling, but the scale factor c shows a dependence on aspect ratio. The dependence of the scale factor on aspect ratio is not surprising, since KBM calculations are highly challenging at low aspect ratio. Confidence in these scaling results is aided by the fact that the same diagnostics, high resolution Thomson scattering systems [19–21], and the same profile fitting code [5] were used in obtaining and analyzing these data. Thus, possible systematic errors due to the use of different diagnostic measurements or different fitting codes are greatly reduced in these comparisons.

3. TESTS OF EPED MODEL FOR PEDESTAL HEIGHT AND WIDTH

The EPED model [15] combines calculated constraints from both PB physics and KBM physics to simultaneously predict pedestal width and pedestal height (for pressure) for Type I ELMing discharges. In this model, pedestal height p_{ped} is defined as $2n_eT_e$. This model has previously been applied to data from a number of machines and found to provide a good prediction of pedestal height in these devices [22]. For the JRT work, significant advances were made in the model and new data sets from C-Mod and DIII-D provided tests of the model in new parameter ranges.

The major advance in the EPED model for the JRT research was to upgrade the way that the constraint of p_{ped} vs. Δ is computed for KBM stability. In the early versions of the model, EPED obtained this constraint from the theoretically motivated relation $\Delta = c(\beta_{\theta,ped})^{1/2}$, discussed previously, where the constant c was taken as 0.076, based on a fit to a DIII-D pedestal database. The approach to calculate pedestal width in the EPED1.6 model is to vary the pedestal height at a given width until the pedestal is found to be at or beyond the threshold for excitation of infinite-n ballooning modes over half of the chosen width, where infinite-n stability is calculated with BALOO [23]. Thus, the upgraded model no longer uses a fitted constant for determination of the width. However, it gives similar results to the original version of the model, implying that the original width scaling is a good approximation to the upgraded model.

The EPED model has been applied to a number of recent discharges from C-Mod [16] and DIII-D [24] in which new data significantly extend the range over which the model has been tested (Fig. 2). Data from C-Mod extended the maximum pedestal pressure by about a factor of two and new data from an upgraded Thomson Scattering system on DIII-D [20] provided new data at large widths. In the new data set, the measured pedestal pressure varies by a factor of about 20 and the quantitative agreement of the predictions with these measurements is typically within 20% or better. These results significantly strengthen confidence in the ability of the EPED model to predict the maximum pedestal pressure

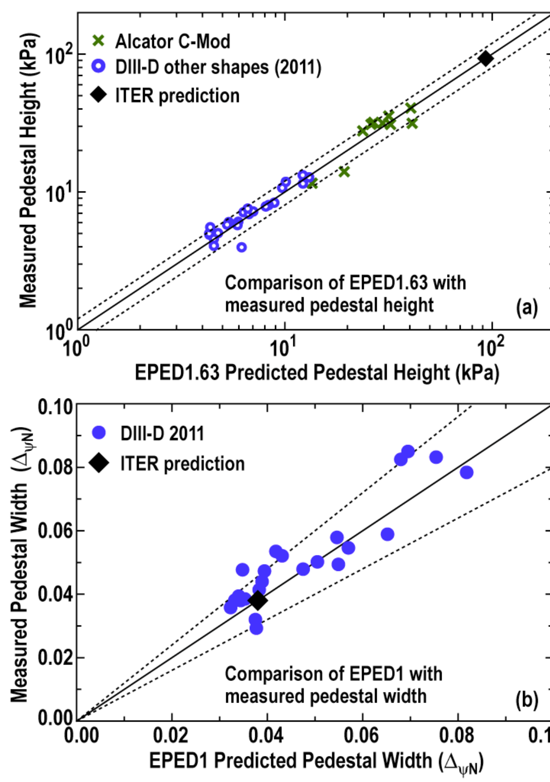

Fig. 2. (a) Measured pedestal pressure height ($2n_eT_e$) vs. predicted height. C-Mod and DIII-D experiment data from 2011. (b) Measured pedestal width (average of n_e and T_e widths) vs predicted width for DIII-D. For (a) and (b), darkest solid line is unity line; upper and lower lines are ±20%.

height in future machines such as ITER. Based on these results, it is reasonable to estimate an error of about 20% in the ability of the model to predict the pedestal pressure height in ITER.

4. SEARCH FOR KBM MODES IN EXPERIMENT AND SIMULATION

Improved confidence that KBMs limit the pressure gradient as assumed in the EPED model requires observation of KBM fluctuations in experiment and confirmation that they have the qualitative and quantitative characteristics predicted from simulations of these modes. Both experimental and simulation work have been performed to address these issues. High frequency coherent (HFC) modes [25], with the characteristics expected for kinetic ballooning modes, have been observed in some conditions in QH-mode discharges. The HFC modes turned on during an increase in the pedestal pressure, which then stopped rising. KBM-like features included a mode frequency of 0.2–0.3 times the ion diamagnetic frequency, a propagation direction in the ion diamagnetic direction in the lab frame, a mode decorrelation rate exceeding the *ExB* shearing rate and a medium-*n* mode number (*n*~10–25). The intensity of broadband density turbulence has also been observed to increase rapidly after an ELM crash [26], as the pedestal pressure is increasing, and to saturate at about the same time as the pedestal pressure saturates. These fluctuations also exhibited characteristics expected for kinetic ballooning modes. Further research is required to determine if the HFC and broadband fluctuations limit the pressure gradient.

Simulations with the electromagnetic gyromagnetic code GYRO [27] have been performed to study the linear physics of KBM modes in a model problem based on a DIII-D pedestal. In the model studies [28], the pressure profile was varied from well below to well above the experimental value and the current density was held at about 80% of the experimental value. The current density was kept low to avoid suppressing infinite-*n* ideal ballooning modes. When run as an eigenmode solver, GYRO calculated the onset of the kinetic ballooning mode at a pressure of about 60% of the experimental pressure (Fig. 3). The BALOO code showed that infinite-*n* ballooning modes had a clear onset at about 70% of the experimental pressure (Fig. 3). Thus, these codes show that the critical gradient for KBM modes is nearly the same as the critical gradient for infinite-*n* ballooning modes, confirming an important assumption in the EPED model. This work supports the plausibility that KBM physics is important in the pedestal structure. However, much additional research remains to address this problem.

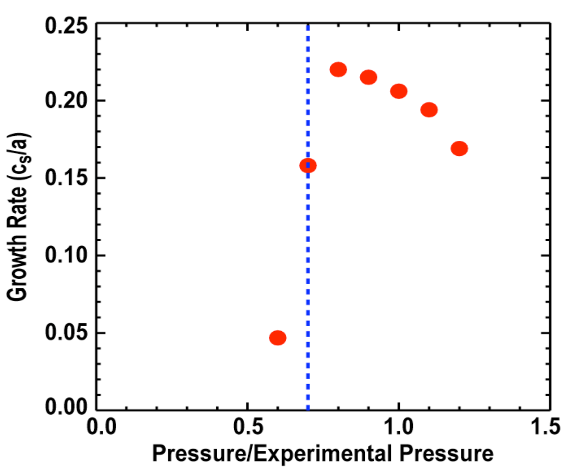

Fig. 3. Linear growth rate for kinetic ballooning mode (in units of ion sound speed over minor radius) as a function of pedestal pressure normalized to the experimental pressure. KBM mode turns on at about 60% of the experimental pressure. Vertical dashed line shows threshold for onset of infinite-n ideal ballooning mode.

5. STUDIES OF TRANSPORT PROCESSES FOR INDIVIDUAL PROFILES

5.1 NEOCLASSICAL TRANSPORT

The XGC0 [12] code has been used to simulate the density pedestal buildup and the model includes combined effects of neoclassical particle transport, due to ion collisions, and neutral fuelling. The code qualitatively reproduces several features of the experiments, including the steep density gradients observed in the H-mode pedestal. Quantitative comparisons to data from C-Mod and DIII-D show that neoclassical transport by itself produces density pedestals that are narrower than observed [29]. Neoclassical transport may be important, but some additional anomalous particle transport is required to explain the observations.

5.2 PALEOCLASSICAL TRANSPORT

Paleoclassical theory [30] predicts that electron thermal transport and particle transport occur due to diffusion of poloidal magnetic flux. An analytic model for T_e and n_e profiles resulting from these transport processes was developed [31] and predictions were compared to measurements in NSTX [32] and DIII-D [33]. The model has made good predictions of the electron thermal diffusivity and the shape of the pedestal density profile in NSTX discharges before and after lithium injection. The model has been evaluated for discharges from all pedestal experiments performed in DIII-D in 2011. The model typically predicts pedestal electron temperature gradients that are close to or larger than observed. Thus, the model predicts the minimum observed electron thermal diffusivity for many cases. In other cases, additional electron thermal transport must be invoked to explain the results. The model predicts densities that are typically about a factor of two times larger than observed in DIII-D. Thus, some additional particle transport must be invoked to explain the observations.

5.3 ELECTRON TEMPERATURE GRADIENT (ETG) TURBULENCE

Short scale turbulence due to electron temperature gradient modes has been proposed as a process to drive electron thermal transport in the steep pedestal [34]. Experiments show some qualitative and quantitative features expected for ETG modes. In all three machines, the ratio of the electron density scale length to the electron temperature scale length (η_e) in the pedestal is observed to be in the range that is expected to drive ETG modes [35]. Short wavelength fluctuations, in a range expected for ETG modes, have been observed at the edge of both NSTX and DIII-D. So far, though, there is no clear measurement of the amount of transport driven by ETG modes. They remain as candidates for electron thermal transport.

5.4 NEUTRAL FUELLING

Fuelling of the pedestal by neutral deuterium atoms has been proposed as a mechanism for controlling the shape of the electron density pedestal, particularly its width [36]. An alternative hypothesis is that plasma transport, such as a particle pinch or neoclassical physics, plays the dominant role in controlling the structure of the density pedestal. At least two modeling activities support the latter hypothesis: (1) analysis of DIII-D data with a model that combines constraints set by particle and momentum balance [37], and (2) analysis of NSTX [32] and DIII-D [33] data with the paleoclassical model in which a pinch is important in the physics of the density profile. On the other hand, there are at least two experimental observations that suggest that neutral fuelling might play an important role. Lithium deposition in NSTX [32,38] reduced the deuterium wall re-cycling coefficient and provided a control for markedly increasing the width and decreasing the gradient of the density pedestal (Fig. 4). An experiment in C-Mod and DIII-D to produce pedestals with the same dimensionless parameters was able to match the T_e profiles but the density profile in DIII-D was somewhat broader than in C-Mod (Fig. 5). An experiment was performed on DIII-D to discriminate between a pinch and fueling by analysis of the rate of rise of the density pedestal [39]. The results show that a pinch is present on top of the pedestal but the physics in the pedestal itself was not resolved. A tentative conclusion from all of these studies is that more than one physics process may be setting the density pedestal structure and the contributions of these processes may vary with experimental conditions.

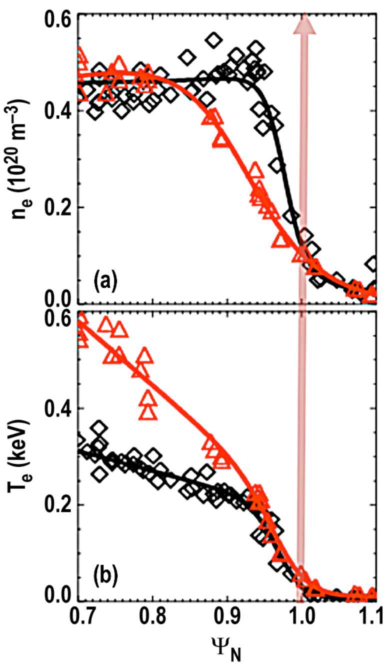

Fig. 4. Profile comparison of no-lithium (black) and with-lithium discharges (red) for (a) n_e, (b) T_e. Application of lithium coatings leads to marked increase in n_e pedestal width with little change in T_e pedestal width.

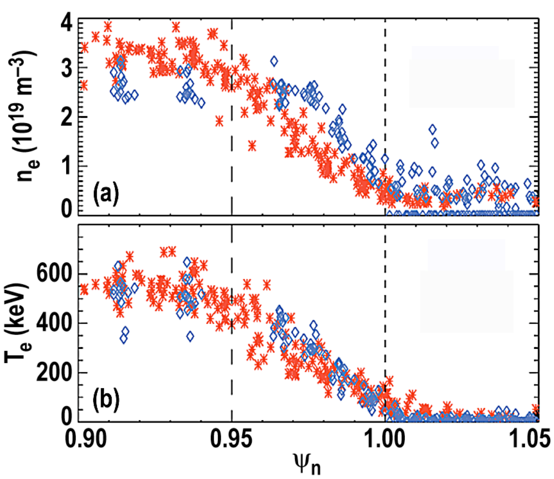

Fig. 5. Pedestal profiles for (a) n_e and (b) T_e from dimensionless matching experiment in C-Mod (blue diamonds) and DIII-D (red stars). The C-Mod data have been appropriately scaled to DIII-D temperatures and densities. There is a near match of both T_e and n_e at normalized $\psi \sim 0.95$. The T_e pedestals overlay well. The DIII-D density pedestal is wider in flux space than in C-Mod density pedestal.

6. SUMMARY AND OUTSTANDING ISSUES

A high level US DOE activity stimulated significant research on pedestal physics in fiscal year 2011. The goal of the research was to identify important physics processes that control pedestal structure and work towards improved predictive capability for these processes. Overall, the results provide increased confidence that several elements of pedestal structure, including peeling-ballooning stability, bootstrap current and pressure gradient limits are sufficiently well understood that good quantitative predictions can be made in many cases, particularly at moderate aspect ratio. Models of these physics processes have been incorporated in the EPED model, which has predicted the pedestal pressure height within an uncertainty of 20% for discharges that span a factor of 20 in pressure. Thus, there is a good basis for predicting pedestal height in future machines, particularly for ITER for which the predicted pressure is an extrapolation of about a factor of 3 from the existing data; this height would be sufficient for ITER to meet its goal. Predictive capability for individual pedestal profiles, which is needed to address other issues of pedestal optimization, remains a major challenge. In this activity, several models for pedestal T_e and n_e profiles were examined. All of these processes remain as candidates for affecting pedestal structure. Thus, correct predictive models of pedestal structure need to self-consistently include multiple physics processes.

REFERENCES

[1] KINSEY, J.E. *et al*., Nucl. Fusion **51** (2011) 083001.

[2] CHAN, V.S. *et al*., Nucl. Fusion **51** (2011) 083019.

[3] SNYDER, P.B. *et al*., Nucl. Fusion **49** (2009) 085035.

[4] LAO, L.L. *et al*., Nucl. Fusion **30** (1990) 1035.

[5] OSBORNE, T.H. *et al*., Journal of Physics: Conf. Series **123** (2008) 012014.

[6] SAUTER O, *et al*., Phys. Plasmas **6** (1999) 2834.

[7] WILSON, H.R. *et al*., Phys. Plasmas **9** (2002) 1277.

[8] BOYLE, D.P. *et al*., Plasma Phys. Control. Fusion **53** (2011) 105011.

[9] HOULBERG, W.A. *et al*., Phys. Plasmas **4** (1997) 3230.

[10] THOMAS, D.M. *et al*., Phys. Plasmas **12** (2005) 056123.

[11] DE BOCK, M.F.M. *et al*., Plasma Phys. Control. Fusion **54** (2012) 025001.

[12] CHANG, C.S. *et al*., Phys. Plasmas **11** (2004) 2649.

[13] BELLI, E.A. and CANDY, J., Plasma Phys. Control. Fusion **50** (2008) 095010.

[14] KOH, S. *et al*., Phys. Plasmas **19** (2012) 072505.

[15] SNYDER, P.B. *et al*., Phys. Plasmas **16** (2009) 056118.

[16] WALK, J.R. *et al*., Nucl. Fusion **52** (2012) 063011.

[17] GROEBNER, R.J. *et al*., Nucl. Fusion **49** (2009) 085037.

[18] DIALLO, A., *et al*., Nucl. Fusion **51** (2011) 103031.

[19] HUGHES, J.W., *et al*., Rev. Sci. Instrum. **74** (2003) 1667.

[20] ELDON, D., *et al*., Rev. Sci. Instrum. **83** (2012) 10E343.

[21] LEBLANC, B.P. *et al*., 2003 Rev. Sci. Instrum. **74** (2003) 1659.

[22] SNYDER, P.B. *et al*., Nucl. Fusion **51** (2011) 103016.

[23] MILLER, R.L. *et al*., Phys. Plasmas **4** (1997) 1062.

[24] SNYDER, P.B. *et al*., Phys. Plasmas **19** (2012) 056115.

[25] YAN, Z. *et al*., Phys. Rev. Lett. **107** (2011) 055004.

[26] YAN, Z. *et al*., Phys. Plasmas **18** (2011) 056117.

[27] CANDY, J and WALTZ, R.E., J. Comput. Phys. **186** (2003) 545.

[28] WANG, E. *et al*., "Linear gyrokinetic analysis of a DIII-D H-mode pedestal near ideal ballooning threshold," accepted for publication in Nucl. Fusion.

[29] PANKIN, A.Y., *et al*., "Kinetic modeling of H-mode pedestal with effects from anomalous transport and MHD stability," Problems of Atomic Science and Technology 2011 No. 1. Series: Plasma Physics (17), p. 8–12.

[30] CALLEN, J.D., Nucl. Fusion **45** (2005) 1120.

[31] CALLEN, J.D. *et al*., Phys. Rev. Lett. **108** (2012) 245003.

[32] CANIK, J.M. *et al*., Phys. Plasmas **18** (2011) 056118.

[33] SMITH, S.P. *et al*., "Comparisons of paleoclassical based pedestal model predictions of electron quantities to measured DIII-D H-mode profiles," accepted for publication in Nucl. Fusion.

[34] JENKO, F. *et al*., Phys. Plasmas **16** (2009) 055901.

[35] GROEBNER, R.J. *et al*., "Empirical study of η_e in H-Mode pedestal in DIII-D," 31st European Physical Society Conf. on Plasma Phys. (Proc. London, 2004) Vol. 28G, EPS (2004) P-2.173.

[36] MAHDAVI, M.A. *et al*., Phys. Plasmas **10** (2003) 3984.

[37] STACEY, W.W. and GROEBNER, R.J., Phys. Plasmas **16** (2009) 102504.

[38] MAINGI, R. *et al*., Nucl. Fusion **52** (2012) 083001.

[39] LEONARD, A.W. *et al*., "Fueling with edge recycling to high density in DIII-D," 20th International Conference on Plasma-Surface Interactions in Controlled Fusion Devices, May 21–25, 2012 in Aachen, Germany, submitted to J. Nucl. Mater.

ACKNOWLEDGMENT

This work was supported in part by the US Department of Energy under DE-FC02-04ER54698, DE-FG02-95ER54309, DE-FG02-00ER54538, DE-AC52-07NA27344, DE-FC02-93ER54186, DE-AC05-00OR22725, DE-AC02-09CH11466, DE-AC04-94AL85000, DE-FG03-94ER54271, DE-FG02-08ER54984, DE-FG02-07ER54917, DE-FC02-05ER54816, DE-FG02-89ER53296, DE-FG02-08ER54999 and work performed at the University of Toronto was funded by the Natural Sciences and Engineering Research Council of Canada.